Isotherm, Kinetics, and Adsorption Mechanism Studies of DTPA-Modified Banana/Pomegranate Peels as Efficient Adsorbents for Removing Cd(II) and Ni(II) from Aqueous Solution

Fanghui Wang
Tianjin University of Science and Technology
Peng Wu
Tianjin University of Science and Technology
Lin Shu
Tianjin University of Science and Technology
Qingbin Guo
Tianjin University of Science and Technology
Di Huang
Nankai University
Huanhuan Liu (lh_tust@tust.edu.cn)
Tianjin University of Science and Technology

Research Article

Keywords: DTPA, modification, fruit peel, adsorption, heavy metal, sewage systems

Posted Date: May 17th, 2021

DOI: https://doi.org/10.21203/rs.3.rs-487875/v1

Version of Record: A version of this preprint was published at Environmental Science and Pollution Research on August 12th, 2021. See the published version at https://doi.org/10.1007/s11356-021-15766-6.

Isotherm, kinetics, and adsorption mechanism studies of DTPA-modified banana/pomegranate peels as efficient adsorbents for removing Cd(II) and Ni(II) from aqueous solution

Fanghui Wang[1,2], Peng Wu[1,2], Lin Shu[1,2], Qingbin Guo[1,2], Di Huang[3,#], Huanhuan Liu[1,2,#]

[1] State Key Laboratory of Food Nutrition and Safety, (Tianjin University of Science & Technology), Tianjin 300457, China.

[2] Key Laboratory of Food Nutrition and Safety, (Tianjin University of Science & Technology), Ministry of Education, Tianjin 300457, China.

[3] TEDA School of Biological Sciences and Biotechnology, Nankai University, TEDA, Tianjin 300457, China.

[#]Correspondence: Di Huang huangdi@nankai.edu.cn

Huanhuan Liu lh_tust@tust.edu.cn

Telephone & Fax +86-22-60912453

Abstract

Two novel absorbents were synthesized for the first time by banana and pomegranate peels using diethylenetriaminepentaacetic acid (DTPA) modification to eliminate Cd(II) and Ni(II) of sewage. The DTPA-modified peels performed significantly higher adsorption capacity than unmodified materials. Adsorption isotherm and kinetics models were simulated to determine their removal efficiency and potential for recovery of these two heavy metals. As the results, the adsorption reached equilibrium within 5 minutes and was well described by the pseudo-second order model and Langmuir isotherm. The surface morphology analysis of the synthetic materials by Scanning Electron Microscopy-Energy Dispersive X-ray spectroscopy, Fourier Transform Infrared spectroscopy and X-ray Photoelectron Spectroscopy, implied that ion exchange, complexation and physical adsorption may together contribute to Cd(II) and Ni(II) loading on DTPA-modified peels. This study demonstrates the feasibility of waste peels as cost-efficient bio-absorbents to remove Cd(II) and Ni(II) in sewage systems, and discovers potential adsorption mechanism of efficiency improvements after DTPA modification.

Keywords: DTPA; modification; fruit peel; adsorption; heavy metal; sewage systems

1. Introduction

Various non-degradable heavy metal ions (HMIs) have received increasing attention on account of their serious threat to the ecosystems and human health by water pollution and food chain accumulation (Haroon et al. 2020, Liu et al. 2012, Nguyen et al. 2021, Oliveira et al. 2021, Zhao et al. 2021). The contamination of cadmium (Cd) and nickel (Ni) have always been a matter of great concern to mankind in many areas(He et al. 2021, Hezarjaribi et al. 2020, Teng et al. 2021). From the current data, the global concentrations of Cd and Ni in rivers and lakes have reached approximately 25.33 and 80.99 μg/L from 2010 to 2017, respectively (Zhou et al. 2020). As one of the most toxic HMIs in wastewater, Cd intake could lead to severe toxicity even at low concentrations (0.001-0.1 mg/L) (Gao et al. 2019), such as infertility, immune deficiency, kidney damage and femoral pain (Ruan et al. 2021), while exposure to Ni could cause allergies and cancer (Yoon et al. 2020). Eliminating Cd and Ni of sewage systems, therefore, becomes an urgent demand to prevent them from entering the human body.

Removal of HMIs by adsorption based on bio-materials, such as agri-wastes, activated sludges, plant tissues and their derivatives, has a broad application due to the low cost, high yield, renewability, less variables to control, and strong metal recovery capacity (Chen et al. 2016, Tan et al. 2016). Fruit peels, feathered with various functional groups (-OH, -COOH, -NH_2, *etc*.) that exist in lignin, cellulose, hemicellulose, pectin and other tissues, can be used as the binding sites of HMIs (Vilardi et al. 2018). Banana and pomegranate are two popular and widely cultivated

fruits in the world. The total production of banana per year is about 1.2×10^8 tons around the world, and the banana peel accounts for 30-40% (Albarelli et al. 2011). In 2017, the world's total pomegranate production was approximately 3.8×10^6 tons and half of pomegranate was composed of peel (El Barnossi et al. 2021). As reported previously, banana and pomegranate peels can be widely used as adsorbents to eliminate HMIs, to maximize the waste utilization and resolve environmental issues. However, the adsorption performance of raw peels was not satisfactory, and thus many chemical treatments were implemented to increase the adsorption capacity, such as acrylonitrile grafted cellulose, carbonization, alkalization and esterification (Zhou et al. 2017). The maximum adsorption capacity of Cd(II) and Ni(II) was only 35.52 and 27.40 mg/g for banana peel (BP) (Memon et al. 2008, Van Thuan et al. 2017), while 22.72 and 10.82 mg/g for pomegranate peel (PP) (Abedi et al. 2016, Khawaja et al. 2015). To further enhance the adsorption performance of agricultural waste peel on HMIs, a low-cost and efficient modification approach needs to be developed.

As a powerful metal chelating agent, diethylenetriaminepentaacetic acid (DTPA) can bind with a variety of metals to form stable complexes, and was frequently employed to enhance the performance of HMI adsorption through chemical modification (Repo et al. 2009, Repo et al. 2010). In this study, DTPA was utilized for the first time to modify banana/pomegranate peel through an esterification reaction with hydroxyl, after defatting and deproteinizing. Abundant-COO from DTPA were loaded to the surface of the adsorbents, providing binding sites for HMIs. To this end, we (1) synthesized two novel bio-adsorbents modified by DTPA to improve the removal

performance of HMIs; (2) optimized the parameters in the adsorption process by adjusting pH, initial concentration, and contact time; (3) explored the potential reaction mechanisms of HMIs loaded onto bio-materials in depth via Electron Microscopy-Energy Dispersive X-ray spectroscopy (SEM-EDX), Fourier Transform Infrared spectroscopy (FTIR) and X-ray Photoelectron Spectroscopy (XPS). This study confirmed the feasibility of developing new bio-based HMI adsorbent with fruit peels and its potential application in agricultural waste treatment and environmental purification.

2 Materials and methods

2.1 Materials and reagents

Banana from Nanning, Guangxi Province, and the pomegranate from Xian, Shaanxi Province of China, were purchased from the local market. The peels were cleaned for five times by deionized water to remove the contaminants attached to the surface, and then dried at 50℃. Next, the obtained peels were cut into small pieces of about 1 cm, then crushed with a grinder and screened using Taylor standard sieve of 40 mush. In this work, reagents for preparing ionic solution were all analytically pure without additional processing, including $Cd(NO_3)_2$ and $Ni(NO_3)_2$, provided by Shanghai Sinopharm Chemical Reagent Co., Ltd. Diethylenetriaminepentaacetic acid (DTPA, purity 99%) and N-N-dimethylformamide (DMF, purity 99.5%) and were provided by ThermoFisher Scientific Co., Ltd. Deionized water (18.25 MΩ cm) was adopted throughout this study.

2.2 Synthesis of DMBP and DMPP

The mercerized peels were prepared by degreasing (Karnitz et al. 2009) and deproteinizing (Pereira et al. 2010), which denoted as mercerized banana peel (MBP) and mercerized pomegranate peel (MPP), respectively. Next, MBP (or MPP) was mixed with DTPA (1:3, w/w) in 42 ml DMF and stirred for 20 h at 75°C. After centrifugation at 10,000×g, the precipitate was successively washed with DMF, deionized water, saturated $NaHCO_3$, deionized water, 95% aqueous ethanol, acetone, respectively. Finally, DTPA modified banana and pomegranate peels (assigned as DMBP and DMPP) were obtained after drying to constant weight in an oven at 50°C.

2.3 Adsorption experiments

The standard solutions (500 mg/L) of Cd(II) and Ni(II) were formulated by dissolving the $Cd(NO_3)_2$ and $Ni(NO_3)_2$ into deionized water, respectively, which were diluted to specified concentrations by deionized water if needed. The effects of pH, initial concentration, contact time and competitive adsorption of Cd(II) and Ni(II) were investigated. 1 M HCl and NaOH were adopted to adjust pH with 3-7. The adsorption isotherms were explored by assessing the loading capacity of Cd(II) and Ni(II) under different initial concentration gradients of Cd(II) (30-250 mg/L) and Ni(II) (20-150 mg/L). The samples of adsorption kinetics experiments were harvested at different time points within 180 min. All batch experiments were performed in Erlenmeyer flasks containing 50 mL HMI solution in a shaker at 200 rpm. Besides, adsorbent dose was maintained at 1 mg/ml, initial ion concentrations at 70 mg/L (Cd(II)) and 50 mg/L (Ni(II)), at 25°C, unless specified otherwise. Next, the mixture of solid and liquid was separated by centrifugation at 10,000×g and filtered with 0.22 μm Nylon filter. Both

initial and residual concentrations of Cd(II) and Ni(II) were detected by an Inductively Coupled Plasma-Atomic Emission Spectroscopy (ICP-OES, Avio 200, PerkinElmer, USA) (Zhang et al. 2020). All these experiments were repeated in triplicate and the equilibrium adsorption capacity (Q_e) was expressed by the Eq. (1).

$$Q_e=(C_0-C_e)V/W \quad (1)$$

Where Q_e is the equilibrium adsorption capacity (mg/g), C_0 and C_e are the initial and equilibrium concentrations of Cd(II) and Ni(II) in solution (mg/L), respectively; V is the solution volume (L), and W is the weight of adsorbent (g).

The adsorption isotherm is modeled by Langmuir (Eq. (2)) and Freundlich (Eq. (3)) isotherm equations and the adsorption kinetic is simulated using pseudo-first-order (Eq. (4)) and pseudo-second-order (Eq. (5)) kinetic equations:

$$C_e/Q_e = 1/(K_c Q_m) + C_e (1/Q_m) \quad (2)$$

$$\log Q_e = \log K_f + (1/n) \log C_e \quad (3)$$

$$\ln(Q_e - Q_t) = \ln Q_e - K_1 t \quad (4)$$

$$t/Q_t = 1/K_2 Q_e^2 + t/Q_e \quad (5)$$

Where Q_m is the maximum adsorption capacity (mg/g) of Cd(II) and Ni(II); K_c (L/mg) is the Langmuir constant associated with adsorption energy; K_f ($L^{1/n}$ $mg^{1-1/n}$ g^{-1}) and 1/n are Freundlich constants related to adsorption capacity and intensity, respectively. Q_t (mg/g) is the amount of Cd(II) and Ni(II) adsorbed at time t (min); K_1 (g mg^{-1} min^{-1}) and K_2 (g mg^{-1} min^{-1}) are the adsorption rate constants of pseudo-first-order and pseudo-second-order adsorption, respectively.

The dimensionless separation constant R_L is often employed to characterize the

Langmuir adsorption isotherm, which can be used to judge whether the adsorption process is favorable. When $R_L = 0$, the adsorption is irreversible; when $0 < R_L < 1$, the reaction is favorable; the reaction is unfavorable when $R_L > 1$, and R_L can be expressed by the following equation:

$$R_L = 1/(1+K_c C_0) \quad (6)$$

2.4 Surface characterization

The surface features of the adsorbents were characterized by a field emission high resolution Scanning Electron Microscope (SEM; Apreo, FEI Inc., USA), equipped with EDX for semi-quantitative elemental analysis (Zhang et al. 2018). The information of surface functional groups was detected by Fourier Transform Infrared spectroscopy (FTIR; Nicolet IS50, ThermoFisher Scientific Inc., USA) within 4000-400 cm^{-1} with a resolution of 4 cm^{-1} (Huang et al. 2019). Composition and binding states of major elements were acquired using X-ray Photoelectron Spectroscopy (XPS; ESCALAB 250Xi, ThermoFisher Scientific Inc., USA). The C1s peak at 284.8 eV was performed as the standard of calibration (Ding et al. 2020).

3 Results and discussion

3.1 Adsorption experiments

3.1.1 Modified banana and pomegranate peels improved HMI removal efficiency

As presented in Fig. 1, the removal rate of unmodified peels on Cd(II) and Ni(II) were intensely limited, especially for pomegranate peel (33.23% and 32.50% for UBP; only 8.84%, 8.67% for UPP). Therefore, a series of modification operations including mercerization and esterification reaction were performed to release -OH and introduce

-COO groups onto the material surface. It was clear that the removal rate to Cd(II) and Ni(II) were significantly increased by 11.22% and 4.76%, to 44.45% and 37.26% for DMBP, while increased by 19.40% and 18.24%, to 28.24% and 26.91% for DMPP. Obviously, the adsorption effect of Cd(II) and Ni(II) on DMBP is more favorable than that on DMPP, and the removal rate of both materials on Cd(II) is much higher than Ni(II).

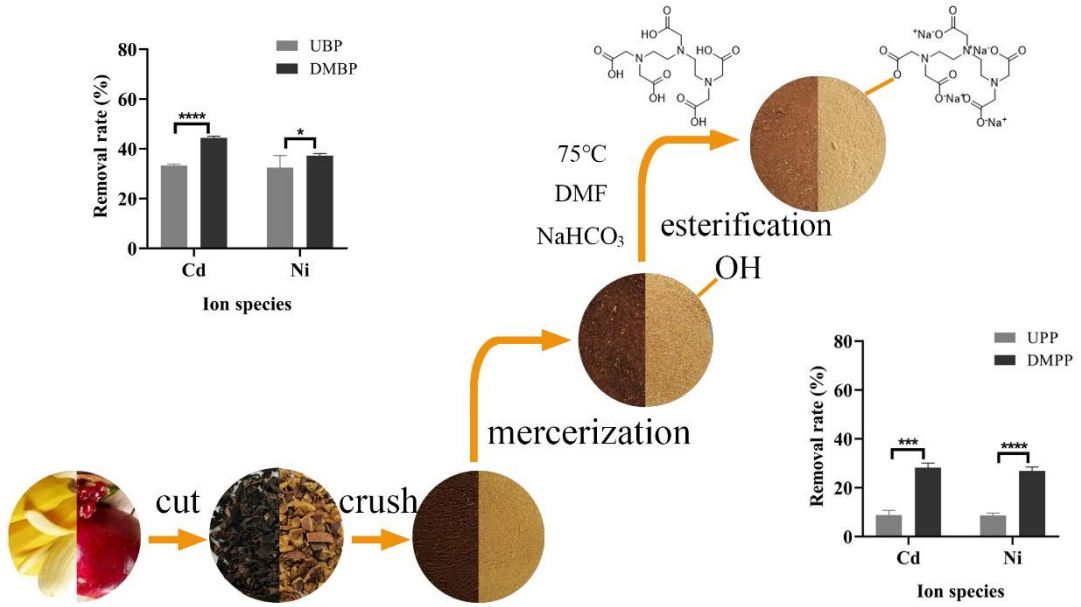

Fig. 1 The fabrication of DTPA modified material composites and the removal rate before and after modification. UBP, unmodified banana peel; DMBP, DTPA modified banana peel; UPP, unmodified pomegranate peel; DMPP, DTPA modified pomegranate peel. * $p<0.05$, *** $p<0.001$, **** $p<0.0001$

3.1.2 Effect of initial pH

The effects of initial pH on the adsorptive performance of DMBP and DMPP were explored. pH 3-7 was selected since the alkaline conditions could induce ion precipitation (Zhang et al. 2020). As depicted in Fig. 2 a, DMBP and DMPP exhibited

poor loading capacities of Cd(II) and Ni(II) at pH 3, which may be ascribed to that the existence of large quantity of protons compete with HMIs for binding sites (Bulin et al. 2020, Zhang et al. 2021). The adsorption capacity gradually increased with the pH from 3 to 6, whereas a downward trend in Cd(II)-adsorption curve appeared at pH=7. Meanwhile, the removal efficiency of both materials for Cd(II) was more excellent than Ni(II), and DMBP has better adsorption performance for Cd(II) and Ni(II).

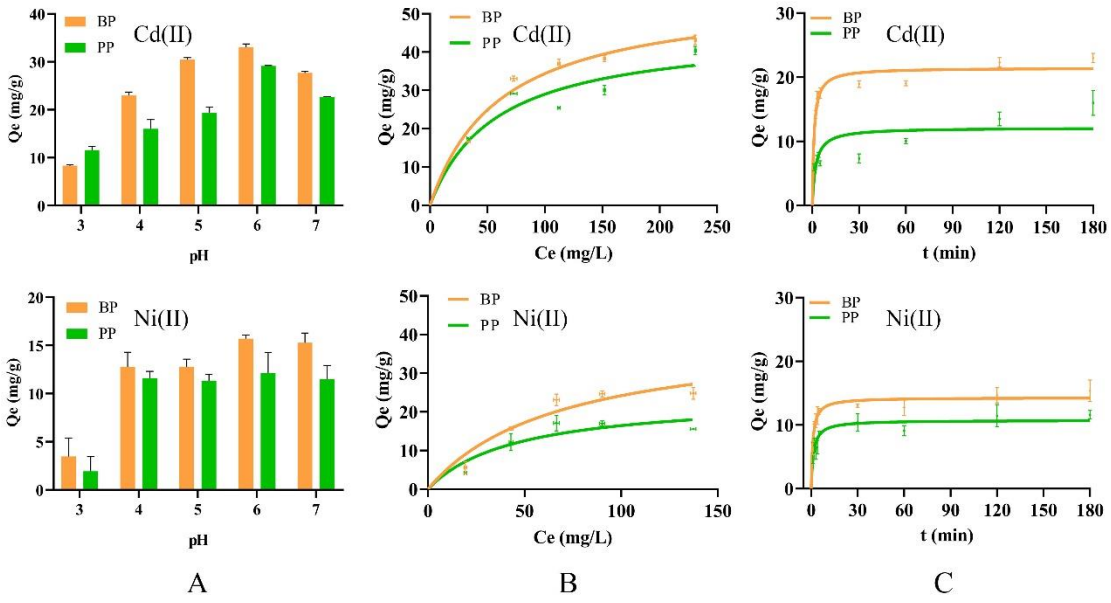

Fig. 2 Effects of solution pH, initial concentration, contact time on adsorption capacity. (a) banana peel (BP) and pomegranate peel (PP) under different pH. (b) Initial concentrations at the optimal pH. (c) Contact time at optimal pH

3.1.3 Effect of initial concentration and isotherm models

The effects of the initial concentration on the adsorption of Cd(II) and Ni(II) were investigated by changing Cd(II) and Ni(II) concentrations. As presented in Fig. 2 b, the adsorbed Cd(II) and Ni(II) contented on DMBP and DMPP were increased as initial concentrations in the aqueous solution increased, which confirmed the excellent adsorption performance. Specifically, the adsorption capacities of the adsorbents

climbed rapidly at lower concentrations and then slowed down to reach equilibrium as the initial concentration of HMIs increased. The outstanding loading capability of both materials suggested the high feasibility of utilizing peel wastes to produce effective adsorbents for HMI cleaning.

Langmuir and Freundlich isotherm models were applied to assess the relationship between loading capacity and initial concentrations. As shown in the model parameters in Table 1, the correlation coefficients R^2 of the Langmuir isotherm model were 0.974-0.998, which were higher than those of the Freundlich model (R^2 were 0.757-0.874), indicating that the adsorption of DMBP and DMPP on Cd(II) and Ni(II) might be monolayer and homogeneous (Yuan et al. 2017). In this work, the values of K_c were 0.037-0.250 for DMBP and DMPP, and the values of R_L were between 0–1, suggesting that the adsorption of Cd(II) and Ni(II) on both materials were favorable. Furthermore, the calculated Q_m of Cd(II) and Ni(II) for DMBP were 46.729 and 29.240 mg/g, respectively, while 46.296 and 16.611 mg/g for DMPP (Table 1), significantly higher than the previous researches (Abedi et al. 2016, Khawaja et al. 2015, Memon et al. 2008, Van Thuan et al. 2017).

Table 1 Parameters of the Langmuir and Freundlich isotherm models in single ion system under different initial concentrations

Adsorbents	Metal ion	Langmuir parameters			Freundlich parameters		
		Q_m (mg/g)	K_c (L/mg)	R^2	K_F ($L^{1/n}$ $mg^{1-1/n}$ g^{-1})	1/n	R^2
BP	Cd(II)	46.729	0.054	0.995	6.926	0.367	0.778
PP		46.296	0.037	0.998	8.202	0.286	0.757
BP	Ni(II)	29.240	0.060	0.979	1.250	0.695	0.797
PP		16.611	0.250	0.974	0.448	0.894	0.874

3.1.4 Effect of contact time and kinetic models

To investigate the adsorption kinetics of the adsorbents (DMBP and DMPP) on Cd(II) and Ni(II), a time-coursed adsorption experiments were performed (Fig. 2 c), and the obtained kinetic data were fitted by the pseudo-first-order and pseudo-second-order kinetic models, which were displayed in Table 2. The adsorption process reached equilibrium within 5 min, which was much faster than previous studies (at least 60 min) (Abedi et al. 2016, Khawaja et al. 2015). The combination of rapid adsorption and high adsorption capacities demonstrated that DMBP and DMPP were desirable for HMI removal.

As shown in Table 2, for both DMBP and DMPP, the values of the correlation coefficient (R^2) calculated from the pseudo-second-order kinetic model (R_2^2 = 0.994-1) were larger than that from the pseudo-first-order kinetic model (R_1^2 =0.825-0.936), and the theoretical values of Q_e were closer to the actual measured values. This phenomenon suggested that the adsorption process could be better described by the pseudo-second-order model. As we all know, the pseudo-first-order model representatives the physical adsorption that the diffusion between the adsorbate and the binding sites dominants the adsorption rate, while the pseudo-second-order model reveals the chemical adsorption such as ion exchange and covalent bonding (Hydari et al. 2012). The better fitting with the pseudo-second-order model indicated that the capture behaviors of both DMBP and DMPP towards Cd(II) and Ni(II) were dominated by chemical adsorption.

Table 2 Kinetics parameters for the adsorption of Cd(II) and Ni(II) on DMBP and DMPP

Adsorbent	Metal ion	Pseudo-first order			Pseudo-second order		
		Q_e	K_1 (g mg^{-1}	R_1^2	Q_e	K_2 (g mg^{-1}	R_2^2

		(mg/g)	min^{-1})		(mg/g)	min^{-1})	
BP	Cd(II)	8.15	0.019	0.854	25.641	0.217	1
PP		9.920	0.011	0.936	37.037	0.055	0.999
BP	Ni(II)	5.073	0.016	0.825	15.267	0.022	0.996
PP		5.121	0.028	0.856	11.655	0.024	0.994

3.1.5 Mixed competitive adsorption

To compare the adsorption effects of DMBP and DMPP on Cd(II) and Ni(II), a mixed adsorption experiment was implemented. The loading capacities of DMBP and DMPP for Cd(II) were stronger than Ni(II) in the mixed ion solution (Fig. 3), demonstrating that DMBP and DMPP had higher absorptivity to Cd(II) than Ni(II), which were consistent with previous results (Cutillas-Barreiro et al. 2016, Liu et al. 2013, Wen &Hu 2021). Moreover, the amount of HMIs captured by DMBP and DMPP in the mixed solution of Cd(II) and Ni(II) was close to the maximum loading capacity in the presence of a single Cd(II), suggesting that the binding sites were fully occupied.

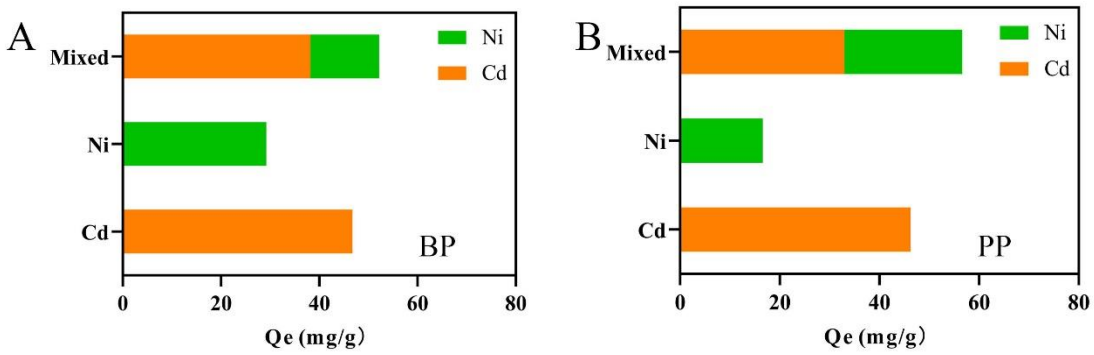

Fig. 3 Comparison of the mixed ion adsorption and the single ion adsorption. (a) banana peel; (b) pomegranate peel. pH =6, C_0 of each HMI is 100 mg/L

3.2 Surface characterization

SEM-EDX system was adopted to observe the changes of physical morphology and elemental composition of the adsorptive materials before and after modification. As shown in Fig. 4, the relatively smooth surface can be seen in unmodified peels (UBP

and UPP). As lipids and proteins were removed after degreasing and deproteinizing, more developed pores and irregularly wrinkled structures were generated to capture metal ions (DMBP and DMPP). The EDX spectrum demonstrated that the major elements of UBP and UPP were C, O, P, Cl and K (Fig. 5 a, d). The disappearance of trace elements such as P, Cl, K and the increase of Na element illustrated the success of mercerization and DTPA modification (Fig. 5 b, e). The contents of Cd and Ni on the surface of DMBP-Ions and DMPP-Ions (Fig. 5 c, f) significantly increased, while the Na content diminished after adsorption, clearly demonstrating that Cd(II) and Ni(II) were successfully captured onto DMBP and DMPP probably by ion exchange with Na(I) (Shen et al. 2021).

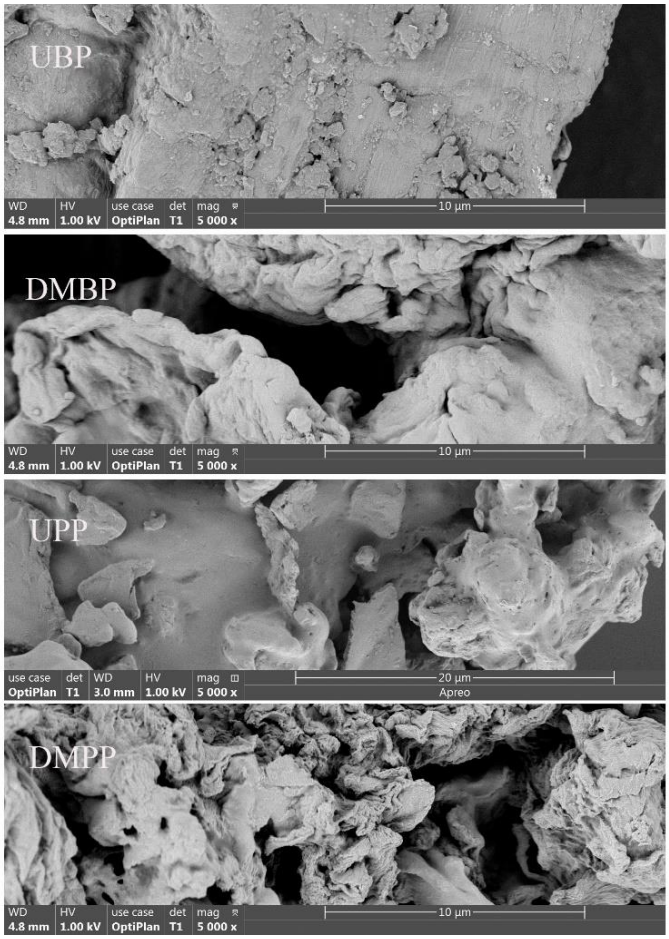

Fig. 4 Surface morphology characterization of the adsorbents by SEM

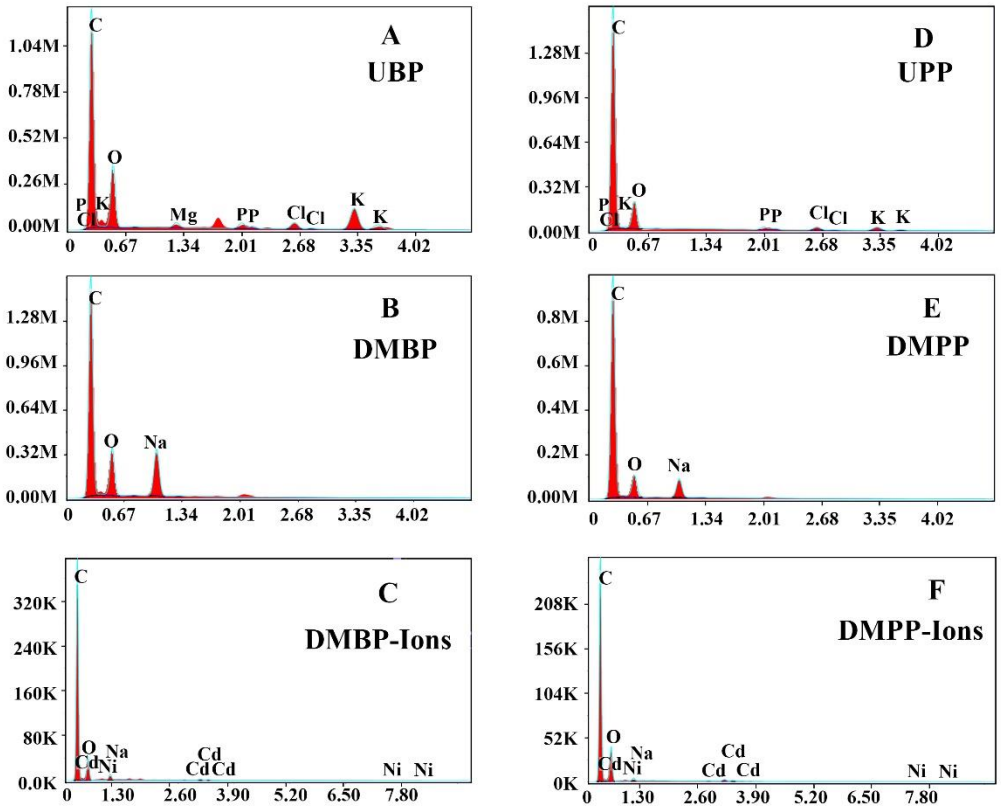

Fig. 5 Surface metal ion states of the adsorbents observed by EDX. (a, d) unmodified peels, (b, e) DTPA modified peels before adsorption, (c, f) DTPA modified peels after adsorption

FTIR spectrum was analyzed for investigating the varieties of surface functional groups before and after modification and adsorption, which was displayed in Fig. 6. In UBP and UPP, the peaks near 3416 and 3415 cm^{-1} (Fig.6 a, b) were detected, corresponding to –OH stretching vibration (Chen et al. 2020). Meanwhile, the signals around 2920 and 2921 cm^{-1} were observed, represented the stretching vibration of C-H (Lessa et al. 2017). The stretching vibration of C=O at 1617 cm^{-1} confirmed the presence of acidic oxygen-containing groups in the adsorbents, which might contribute to the HMI adsorption (Fan et al. 2020). The peaks at 1037 and 1049 cm^{-1} were attributed to C-O stretching (Shen et al. 2021), and the bands around 1734 and 1732 cm^{-1} were ascribed to N-H stretching. After mercerization, the disappearance of N-H

signal probably was caused by the removal of protein, meanwhile, the reduction of C-H and C=O peak area might be attributed to the degreasing treatment. Moreover, the increase of peak intensity at 1037 and 1049 cm^{-1} illustrated the increase in the proportion of cellulose in MBP and MPP, which provided another evidence for the effectiveness of mercerization (Zhang et al. 2018). After modification with DTPA, the peaks around 1628 and 1020 cm^{-1} were broadened, which suggested that DTPA was successfully grafted onto the materials and large quantities of –COO were introduced, providing more binding sites for the capture of Cd(II) and Ni(II). After binding with HMIs, blue shift of C=O and C-O peaks occurred (from 1628 cm^{-1} and 1020 cm^{-1} to 1630 cm^{-1} and 1023 cm^{-1} for DMBP, from 1629 and 1025 cm^{-1} to 1636 and 1050 cm^{-1} for DMPP, respectively), which might be due to the interaction between high electron density of HMIs and oxygen-containing groups (Ding et al. 2016). Meanwhile, the reduction of the peak area near 3440, 1630 and 1020 also provided a theoretical basis for the surface complexation between these oxygen-containing groups and metal ions.

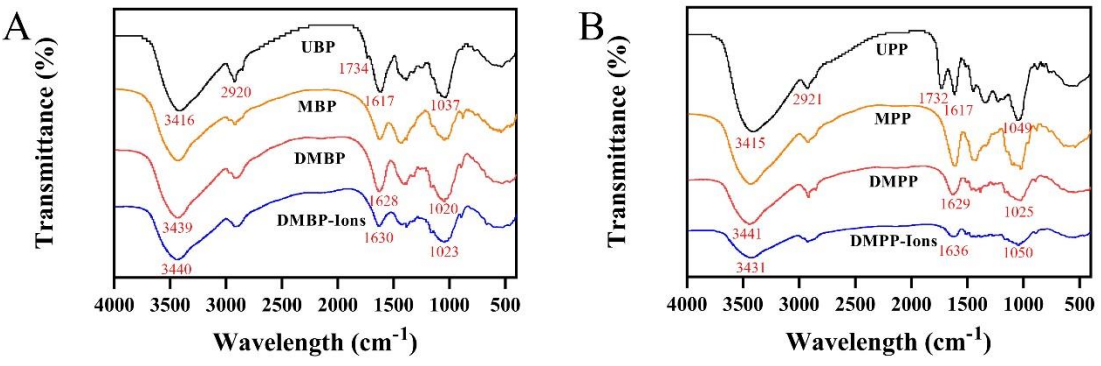

Fig. 6 FTIR spectra of the adsorbents. MBP (mercerized banana peel), MPP (mercerized pomegranate peel)

From the EDX results (Fig. 5 c, f), new peaks of Cd and Ni appeared in DMBP-

296 Ions and DMPP-Ions after adsorption, suggesting that Cd(II) and Ni(II) were
297 successfully loaded onto DMBP and DMPP. Subseqently, in order to further explore the
298 changes of surface chemical composition of DMBP and DMPP before and after
299 adsorption, XPS spectrum was recorded. From the full spectrum (Fig. 7 a), two new
300 peaks of Cd and Ni obviously occurred after binding with HMIs, implying that
301 abundant Cd(II) and Ni(II) were loaded onto DMBP and DMPP. Particularly, the peaks
302 observed around 412, 405 eV and 860, 856 eV in Fig. 7 b were attributed to Cd 3d and
303 Ni 2p, respectively (Chada et al. 2005, Ding et al. 2020). The intensity of Ni 2p was
304 weaker than Cd 3d, verifying the lower adsorption of Ni(II) mentioned above (Fig. 2).
305 Furthermore, the spectrum of C 1s was split into three peaks around 285, 286 and 288
306 eV (Fig. 7 c), representing C–C, C–O and C=O peaks, separately (He et al. 2014, Lyu
307 et al. 2017). Each peak expressed a slight variation after Cd(II) and Ni(II) adsorption
308 (286.6/286.4 to 286.4/286.5 and 288.3/288.2 to 287.9/288.1 for DMBP/DMPP,
309 respectively), implying that the abundant oxygen-containing groups such as -OH and -
310 COOH on the both materials surface could bind with Cd(II) and Ni(II) to form
311 complexes. Furthermore, from the high-resolution O 1s of the adsorbents (Fig. 7 c), the
312 binding energy of C=O could be observed around 532 eV , which exhibited minor
313 changes after Cd(II) and Ni(II) adsorption (Pang et al. 2019), indicating these oxygen-
314 containing functional groups successfully participated in the complexation. The peak
315 intensity of Na 1s around 1071 eV evidently decreased after adsorption, verified the
316 conlusion from EDX analysis that ion exchange between Na(I) with Cd(II) and Ni(II)
317 may occur in the adsorption process. All these above results suggested that chemical

adsorption played a crucial part in the adsorption process of Cd(II) and Ni(II), flowed by physical adsorption.

In summary, DTPA modified banana and pomegranate peels exhibitted efficient adsorption potential for the elimination of Cd(II) and Ni(II) from the sewage system, and the complexity of DMBP and DMPP resulted in multi-adsorption mechanisms of Cd(II) and Ni(II), including surface complexation, ion exchange and physical adsorption. In detail, abundant oxygen-containing groups such as hydroxyl and carboxyl groups might generate complex complexes with Cd(II) and in the form of C-O-M (M represented Cd and Ni) (Zhang et al. 2020), which can be manifested from the change of -OH, C-O, C=O in FTIR spectrum and the shift of C-O and C=O in XPS. As seen in EDX and XPS spectrum, the significant reduction in Na content of both samples can explain that the free Cd(II) and Ni(II) might be substituted by –COO…Na…COO–. Furthermore, it was noteworthy that DTPA modified materials exhibited shrunk and loose morphology observed by SEM, indicating physical adsorption may also be involved in adsorption process.

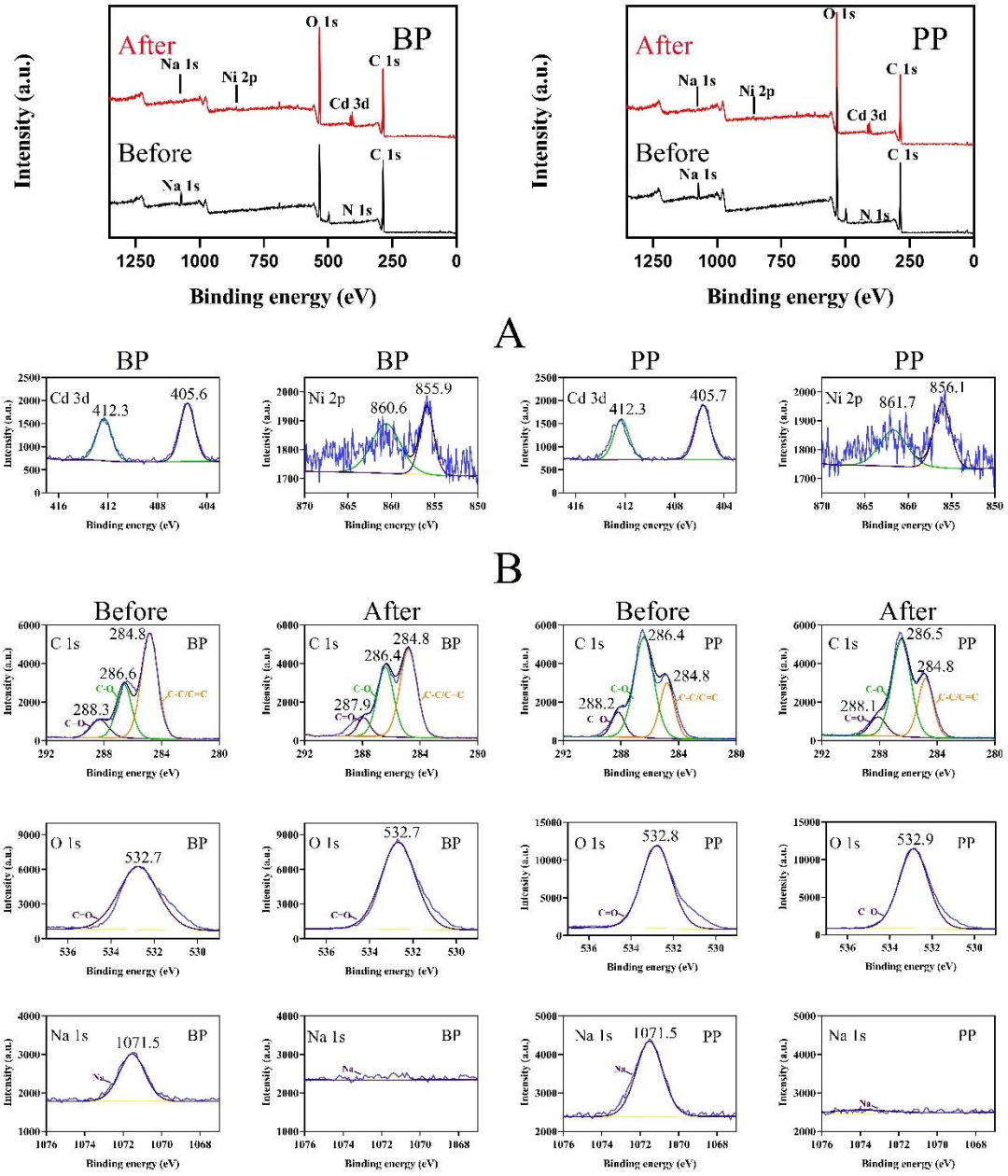

334 **Fig. 7** High-resolution XPS spectra of adsorbents. (a) full spectrum of adsorbents before and after
335 adsorption, (b) fine spectrum of Cd and Ni after adsorption; (c) fine spectrum of C, O, Na before
336 and after adsorption

337 **4. Conclusion**

338 Two novel adsorbents were prepared by mercerizing and then esterification using
339 DTPA for the first time. Compared with UBP/UPP, DMBP/DMPP performed greater

adsorption capacities (46.729/46.296 mg/g for Cd(II), and 29.240/16.611 mg/g for Ni(II)), which could be employed as efficient adsorbents to remove HMIs from sewage. The entire adsorption reached equilibrium within 5 min, and the adsorption process was well fitted with Langmuir isotherm model and the pseudo-second order equation. Adsorption mechanisms mainly include ion exchange with Na(I), complexation with the surface of oxygen-containing groups and physical adsorption. This work reveals that DTPA esterification is a potential treatment mean to prepare high-efficient and low-cost adsorbent from agricultural wastes for removing Cd(II) and Ni(II) from sewage.

Declarations

Funding This work was supported by the National Natural Science Foundation of China (Grants 31800072, 31970084, 31400081) and the Open Fund of Ministry of Education Key Laboratory of Molecular Microbiology and Technology, Nankai University.

Authors' contributions Fanghui Wang: Conceptualization, Investigation, Data curation, Writing-original draft. Peng Wu: Investigation, Methodology, Writing-original draft. Lin Shu: Investigation, Review. Qingbin Guo: Review. Di Huang: Conceptualization, Supervision, Funding acquisition. Huanhuan Liu: Conceptualization, Supervision, Writing-original draft, Funding acquisition.

Competing interests The authors declare that they have no known competing financial interests or personal relationships that could have appeared to influence the work reported in this paper.

Acknowledgements We gratefully acknowledge the technical supports from Instrument & Testing Center of Tianjin University of Science and Technology.

Ethics approval and consent to participate Not applicable.

Consent for publication Not applicable.

Availability of data and materials The datasets used and/or analyzed during the current study are available from the corresponding author on reasonable request.

Reference

Abedi M, Salmani MH, Mozaffari SA (2016) Adsorption of Cd ions from aqueous solutions by iron modified pomegranate peel carbons: kinetic and thermodynamic studies. International Journal of Environmental Science and Technology. https://doi.org/10.1007/s13762-016-1002-7

Albarelli JQ, Rabelo RB, Santos DT, Beppu MM, Meireles MAA (2011) Effects of supercritical carbon dioxide on waste banana peels for heavy metal removal. The Journal of Supercritical Fluids. https://doi.org/10.1016/j.supflu.2011.07.014

Bulin C, Zhang Y, Li B, Zhang B (2020) Removal performance of aqueous Co(II) by magnetic graphene oxide and adsorption mechanism. Journal of Physics and Chemistry of Solids. https://doi.org/10.1016/j.jpcs.2020.109483

Chada VGR, Hausner DB, Strongin DR, Rouff AA, Reeder RJ (2005) Divalent Cd and Pb uptake on calcite {10$\bar{1}$4} cleavage faces: An XPS and AFM study. Journal of Colloid and Interface Science. https://doi.org/10.1016/j.jcis.2005.03.018

Chen D, Zhang HN, Yang K, Wang HY (2016) Functionalization of 4-aminothiophenol and 3-aminopropyltriethoxysilane with graphene oxide for potential dye and copper removal. Journal of Hazardous Materials. https://doi.org/10.1016/j.jhazmat.2016.02.040

Chen Y, Zeng Z, Li Y, Liu Y, Chen Y, Wu Y, Zhang J, Li H, Xu R, Wang S, Peng Z (2020) Glucose enhanced the oxidation performance of iron-manganese binary oxides: Structure and mechanism of removing tetracycline. Journal of Colloid

391 and Interface Science. https://doi.org/10.1016/j.jcis.2020.04.006
392 Cutillas-Barreiro L, Paradelo R, Igrexas-Soto A, Núñez-Delgado A, Fernández-
393 Sanjurjo MJ, Álvarez-Rodriguez E, Garrote G, Nóvoa-Muñoz JC, Arias-
394 Estévez M (2016) Valorization of biosorbent obtained from a forestry waste:
395 Competitive adsorption, desorption and transport of Cd, Cu, Ni, Pb and Zn.
396 Ecotoxicology and Environmental Safety.
397 https://doi.org/10.1016/j.ecoenv.2016.05.007
398 Ding C, Cheng W, Wang X, Wu ZY, Sun Y, Chen C, Wang X, Yu SH (2016) Competitive
399 sorption of Pb(II), Cu(II) and Ni(II) on carbonaceous nanofibers: A
400 spectroscopic and modeling approach. Journal of Hazardous Materials.
401 https://doi.org/10.1016/j.jhazmat.2016.04.002
402 Ding C, Cheng W, Wang X, Wu Z-Y, Sun Y, Chen C, Wang X, Yu S-H (2020)
403 Corrigendum: Competitive sorption of Pb(II), Cu(II) and Ni(II) on
404 carbonaceous nanofibers: A spectroscopic and modeling approach. Journal of
405 Hazardous Materials. https://doi.org/10.1016/j.jhazmat.2020.122118
406 El Barnossi A, Moussaid F, Iraqi Housseini A (2021) Tangerine, banana and
407 pomegranate peels valorisation for sustainable environment: A review.
408 Biotechnology Reports. https://doi.org/10.1016/j.btre.2020.e00574
409 Fan J, Li Y, Yu H, Li Y, Yuan Q, Xiao H, Li F, Pan B (2020) Using sewage sludge with
410 high ash content for biochar production and Cu(II) sorption. Science of The
411 Total Environment. https://doi.org/10.1016/j.scitotenv.2020.136663
412 Gao LY, Deng JH, Huang GF, Li K, Cai KZ, Liu Y, Huang F (2019) Relative distribution

413 of Cd(2+) adsorption mechanisms on biochars derived from rice straw and
414 sewage sludge. Bioresource Technology.
415 https://doi.org/10.1016/j.biortech.2018.09.138
416 Haroon H, Shah JA, Khan MS, Alam T, Khan R, Asad SA, Ali MA, Farooq G, Iqbal M,
417 Bilal M (2020) Activated carbon from a specific plant precursor biomass for
418 hazardous Cr(VI) adsorption and recovery studies in batch and column reactors:
419 Isotherm and kinetic modeling. Journal of Water Process Engineering.
420 https://doi.org/10.1016/j.jwpe.2020.101577
421 He J, Lu Y, Luo G (2014) Ca(II) imprinted chitosan microspheres: An effective and
422 green adsorbent for the removal of Cu(II), Cd(II) and Pb(II) from aqueous
423 solutions. Chemical Engineering Journal.
424 https://doi.org/10.1016/j.cej.2014.01.096
425 He X, Hong ZN, Jiang J, Dong G, Liu H, Xu RK (2021) Enhancement of Cd(II)
426 adsorption by rice straw biochar through oxidant and acid modifications.
427 Environmental Science and Pollution Research.
428 https://doi.org/10.1007/s11356-021-13742-8
429 Hezarjaribi M, Bakeri G, Sillanpää M, Chaichi MJ, Akbari S (2020) Novel adsorptive
430 membrane through embedding thiol-functionalized hydrous manganese oxide
431 into PVC electrospun nanofiber for dynamic removal of Cu(II) and Ni(II) ions
432 from aqueous solution. Journal of Water Process Engineering.
433 https://doi.org/10.1016/j.jwpe.2020.101401
434 Huang ZQ, Cheng C, Liu ZW, Luo WH, Zhong H, He GC, Liang CL, Li LQ, Deng LQ,

435 Fu W (2019) Gemini surfactant: A novel flotation collector for harvesting of
436 microalgae by froth flotation. Bioresource Technology.
437 https://doi.org/10.1016/j.biortech.2018.12.106
438 Hydari S, Sharififard H, Nabavinia M, Parvizi Mr (2012) A comparative investigation
439 on removal performances of commercial activated carbon, chitosan biosorbent
440 and chitosan/activated carbon composite for cadmium. Chemical Engineering
441 Journal. https://doi.org/10.1016/j.cej.2012.04.057
442 Karnitz O, Gurgel LVA, de Freitas RP, Gil LF (2009) Adsorption of Cu(II), Cd(II), and
443 Pb(II) from aqueous single metal solutions by mercerized cellulose and
444 mercerized sugarcane bagasse chemically modified with EDTA dianhydride
445 (EDTAD). Carbohydrate Polymers.
446 https://doi.org/10.1016/j.carbpol.2009.02.016
447 Khawaja M, Mubarak S, Zia-Ur-Rehman M, Kazi AA, Hamid A (2015) Adsorption
448 studies of pomegranate peel actived charcoal for nickel (II) ion. Journal of The
449 Chilean Chemical Society. https://doi.org/10.4067/s0717-97072015000400003
450 Lessa EF, Gularte MS, Garcia ES, Fajardo AR (2017) Orange waste: A valuable
451 carbohydrate source for the development of beads with enhanced adsorption
452 properties for cationic dyes. Carbohydrate Polymers.
453 https://doi.org/10.1016/j.carbpol.2016.10.019
454 Liu C, Huu Hao N, Guo W, Tung K-L (2012) Optimal conditions for preparation of
455 banana peels, sugarcane bagasse and watermelon rind in removing copper from
456 water. Bioresource Technology. https://doi.org/10.1016/j.biortech.2012.06.004

457 Liu H, Wang C, Liu J, Wang B, Sun H (2013) Competitive adsorption of Cd(II), Zn(II)
458 and Ni(II) from their binary and ternary acidic systems using tourmaline.
459 Journal of Environmental Management.
460 https://doi.org/10.1016/j.jenvman.2013.06.024
461 Lyu H, Tang J, Huang Y, Gai L, Zeng EY, Liber K, Gong Y (2017) Removal of
462 hexavalent chromium from aqueous solutions by a novel biochar supported
463 nanoscale iron sulfide composite. Chemical Engineering Journal.
464 https://doi.org/10.1016/j.cej.2017.04.058
465 Memon JR, Memon SQ, Bhanger MI, Memon GZ, El-Turki A, Allen GC (2008)
466 Characterization of banana peel by scanning electron microscopy and FT-IR
467 spectroscopy and its use for cadmium removal. Colloids and Surfaces B:
468 Biointerfaces. https://doi.org/10.1016/j.colsurfb.2008.07.001
469 Nguyen LH, Van HT, Nguyen QT, Nguyen TH, Nguyen TBL, Nguyen VQ, Bui TU, Le
470 Sy H (2021) Paper waste sludge derived-hydrochar modified by iron (III)
471 chloride for effective removal of Cr(VI) from aqueous solution: Kinetic and
472 isotherm studies. Journal of Water Process Engineering.
473 https://doi.org/10.1016/j.jwpe.2020.101877
474 Oliveira MRF, do Vale Abreu K, Romao ALE, Davi DMB, de Carvalho Magalhaes CE,
475 Carrilho E, Alves CR (2021) Carnauba (Copernicia prunifera) palm tree
476 biomass as adsorbent for Pb(II) and Cd(II) from water medium. Environmental
477 Science and Pollution Research. https://doi.org/10.1007/s11356-020-07635-5
478 Pang H, Diao Z, Wang X, Ma Y, Yu S, Zhu H, Chen Z, Hu B, Chen J, Wang X (2019)

Adsorptive and reductive removal of U(VI) by Dictyophora indusiate-derived biochar supported sulfide NZVI from wastewater. Chemical Engineering Journal. https://doi.org/10.1016/j.cej.2019.02.098

Pereira FV, Gurgel LV, Gil LF (2010) Removal of Zn^{2+} from aqueous single metal solutions and electroplating wastewater with wood sawdust and sugarcane bagasse modified with EDTA dianhydride (EDTAD). Journal of Hazardous Materials. https://doi.org/10.1016/j.jhazmat.2009.11.115

Repo E, Kurniawan TA, Warchol JK, Sillanpää MET (2009) Removal of Co(II) and Ni(II) ions from contaminated water using silica gel functionalized with EDTA and/or DTPA as chelating agents. Journal of Hazardous Materials. https://doi.org/10.1016/j.jhazmat.2009.06.111

Repo E, Warchol JK, Kurniawan TA, Sillanpää MET (2010) Adsorption of Co(II) and Ni(II) by EDTA- and/or DTPA-modified chitosan: Kinetic and equilibrium modeling. Chemical Engineering Journal. https://doi.org/10.1016/j.cej.2010.04.030

Ruan S-L, Xie L, Ou J-W, Sun X-S, Zhang Y-P, Hu J-R (2021) Molecular cloning, the characterization of metallothionein and catalase, and the evaluation of testicular toxicity of Cd in the Chinese fire-bellied newt (Cynops orientalis). Ecotoxicology and Environmental Safety. https://doi.org/10.1016/j.ecoenv.2020.111731

Shen Y, Guo JZ, Bai LQ, Chen XQ, Li B (2021) High effective adsorption of Pb(II) from solution by biochar derived from torrefaction of ammonium persulphate

pretreated bamboo. Bioresource Technology. https://doi.org/10.1016/j.biortech.2020.124616

Tan IAW, Chan JC, Hameed BH, Lim LLP (2016) Adsorption behavior of cadmium ions onto phosphoric acid-impregnated microwave-induced mesoporous activated carbon. Journal of Water Process Engineering. https://doi.org/10.1016/j.jwpe.2016.10.007

Teng Y, Jiang Z, Yu A, Yu H, Huang Z, Zou L (2021) Optimization of preparation parameters for environmentally friendly attapulgite functionalized by chitosan and its adsorption properties for Cd^{2+}. Environmental Science and Pollution Research. https://doi.org/10.1007/s11356-021-13788-8

Van Thuan T, Quynh BTP, Nguyen TD, Ho VTT, Bach LG (2017) Response surface methodology approach for optimization of Cu^{2+}, Ni^{2+} and Pb^{2+} adsorption using KOH-activated carbon from banana peel. Surfaces and Interfaces. https://doi.org/10.1016/j.surfin.2016.10.007

Vilardi G, Di Palma L, Verdone N (2018) Heavy metals adsorption by banana peels micro-powder: Equilibrium modeling by non-linear models. Chinese Journal of Chemical Engineering. https://doi.org/10.1016/j.cjche.2017.06.026

Wen J, Hu X (2021) Metal selectivity and effects of co-existing ions on the removal of Cd, Cu, Ni, and Cr by ZIF-8-EGCG nanoparticles. Journal of Colloid and Interface Science. https://doi.org/10.1016/j.jcis.2021.01.021

Yoon K, Cho D-W, Bhatnagar A, Song H (2020) Adsorption of As(V) and Ni(II) by Fe-Biochar composite fabricated by co-pyrolysis of orange peel and red mud.

Environmental Research. https://doi.org/10.1016/j.envres.2020.109809

Yuan G, Tian Y, Liu J, Tu H, Liao J, Yang J, Yang Y, Wang D, Liu N (2017) Schiff base anchored on metal-organic framework for Co(II) removal from aqueous solution. Chemical Engineering Journal. https://doi.org/10.1016/j.cej.2017.06.024

Zhang W, Deng Q, He Q, Song J, Zhang S, Wang H, Zhou J, Zhang H (2018) A facile synthesis of core-shell/bead-like poly (vinyl alcohol)/alginate@PAM with good adsorption capacity, high adaptability and stability towards Cu(II) removal. Chemical Engineering Journal. https://doi.org/10.1016/j.cej.2018.06.129

Zhang W, Song J, He Q, Wang H, Lyu W, Feng H, Xiong W, Guo W, Wu J, Chen L (2020) Novel pectin based composite hydrogel derived from grapefruit peel for enhanced Cu(II) removal. Journal of Hazardous Materials. https://doi.org/10.1016/j.jhazmat.2019.121445

Zhang Z, Wang T, Zhang H, Liu Y, Xing B (2021) Adsorption of Pb(II) and Cd(II) by magnetic activated carbon and its mechanism. Science of The Total Environment. https://doi.org/10.1016/j.scitotenv.2020.143910

Zhao N, Zhao C, Tsang DCW, Liu K, Zhu L, Zhang W, Zhang J, Tang Y, Qiu R (2021) Microscopic mechanism about the selective adsorption of Cr(VI) from salt solution on O-rich and N-rich biochars. Journal of Hazardous Materials. https://doi.org/10.1016/j.jhazmat.2020.124162

Zhou N, Chen HG, Xi JT, Yao DH, Zhou Z, Tian Y, Lu XY (2017) Biochars with excellent Pb(II) adsorption property produced from fresh and dehydrated

545 banana peels via hydrothermal carbonization. Bioresource Technology.
546 https://doi.org/10.1016/j.biortech.2017.01.074
547 Zhou Q, Yang N, Li Y, Ren B, Ding X, Bian H, Yao X (2020) Total concentrations and
548 sources of heavy metal pollution in global river and lake water bodies from 1972
549 to 2017. Global Ecology and Conservation.
550 https://doi.org/10.1016/j.gecco.2020.e00925
551

Figures

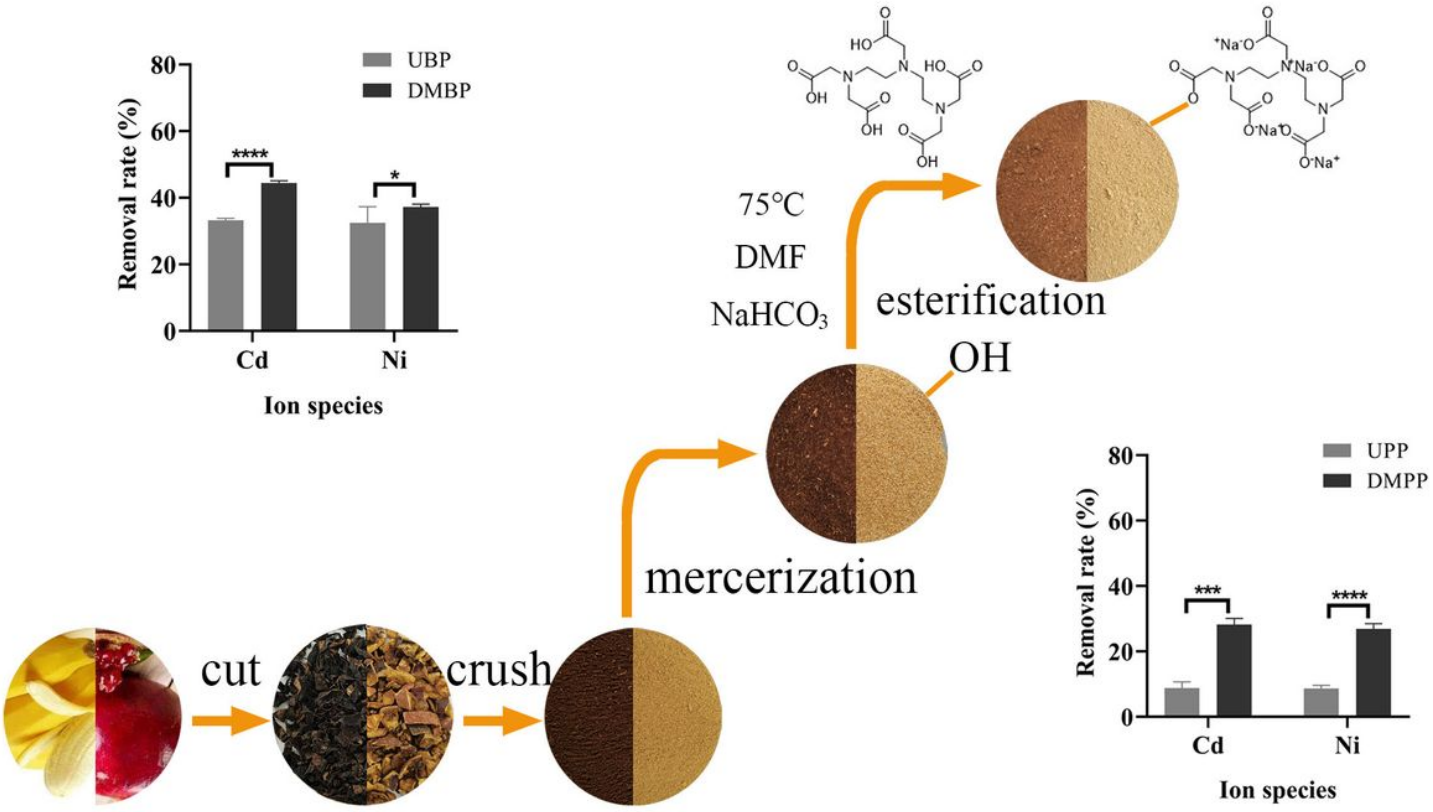

Figure 1

The fabrication of DTPA modified material composites and the removal rate before and after modification. UBP, unmodified banana peel; DMBP, DTPA modified banana peel; UPP, unmodified pomegranate peel; DMPP, DTPA modified pomegranate peel. * $p<0.05$, *** $p<0.001$, **** $p<0.0001$

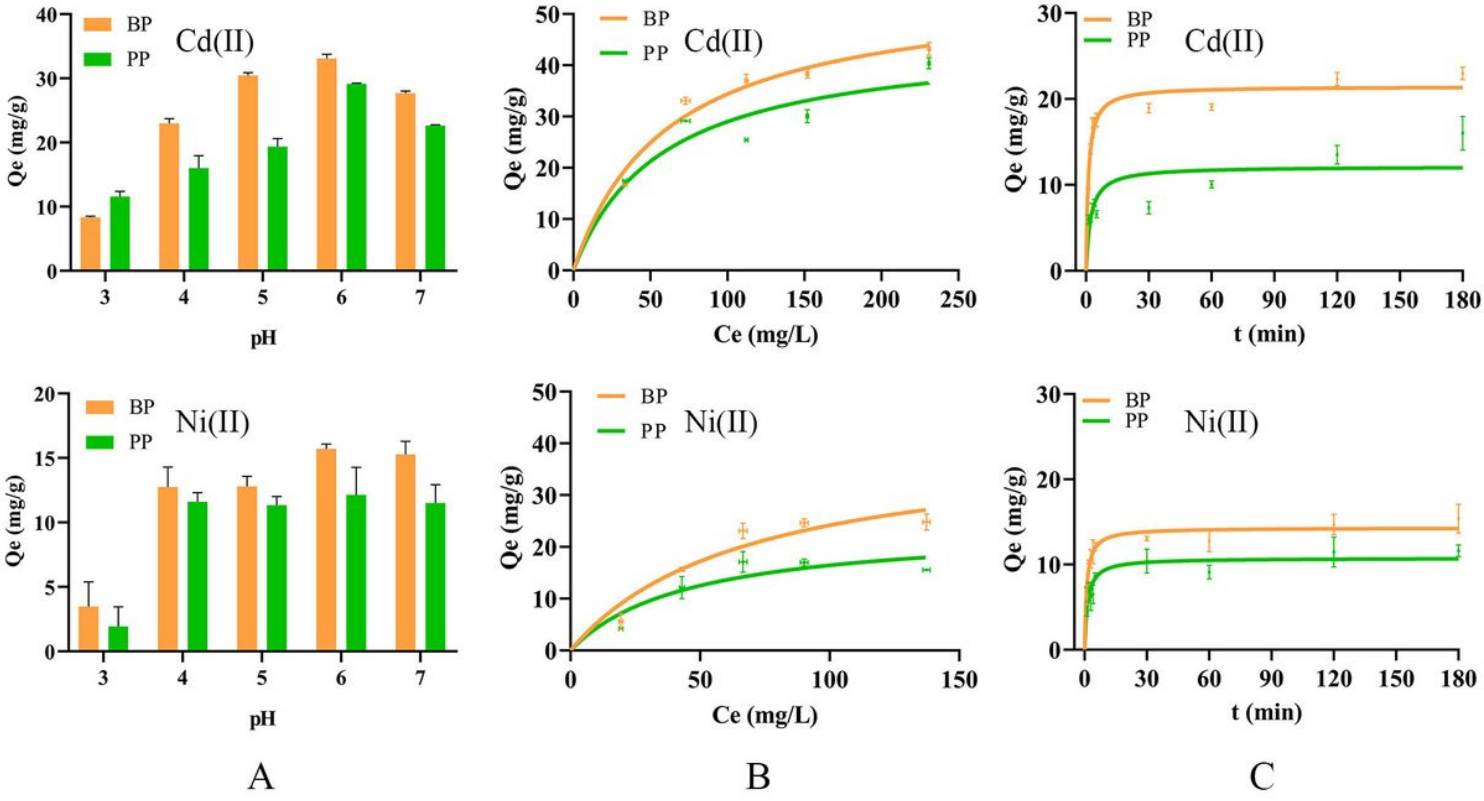

Figure 2

Effects of solution pH, initial concentration, contact time on adsorption capacity. (a) banana peel (BP) and pomegranate peel (PP) under different pH. (b) Initial concentrations at the optimal pH. (c) Contact time at optimal pH

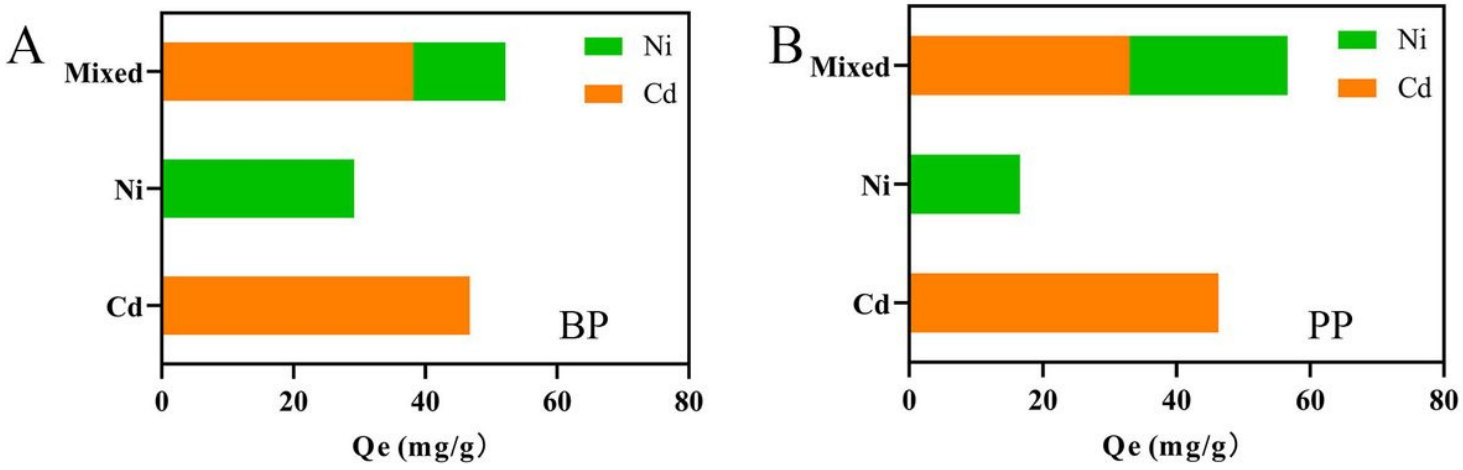

Figure 3

Comparison of the mixed ion adsorption and the single ion adsorption. (a) banana peel; (b) pomegranate peel. pH =6, C0 of each HMI is 100 mg/L

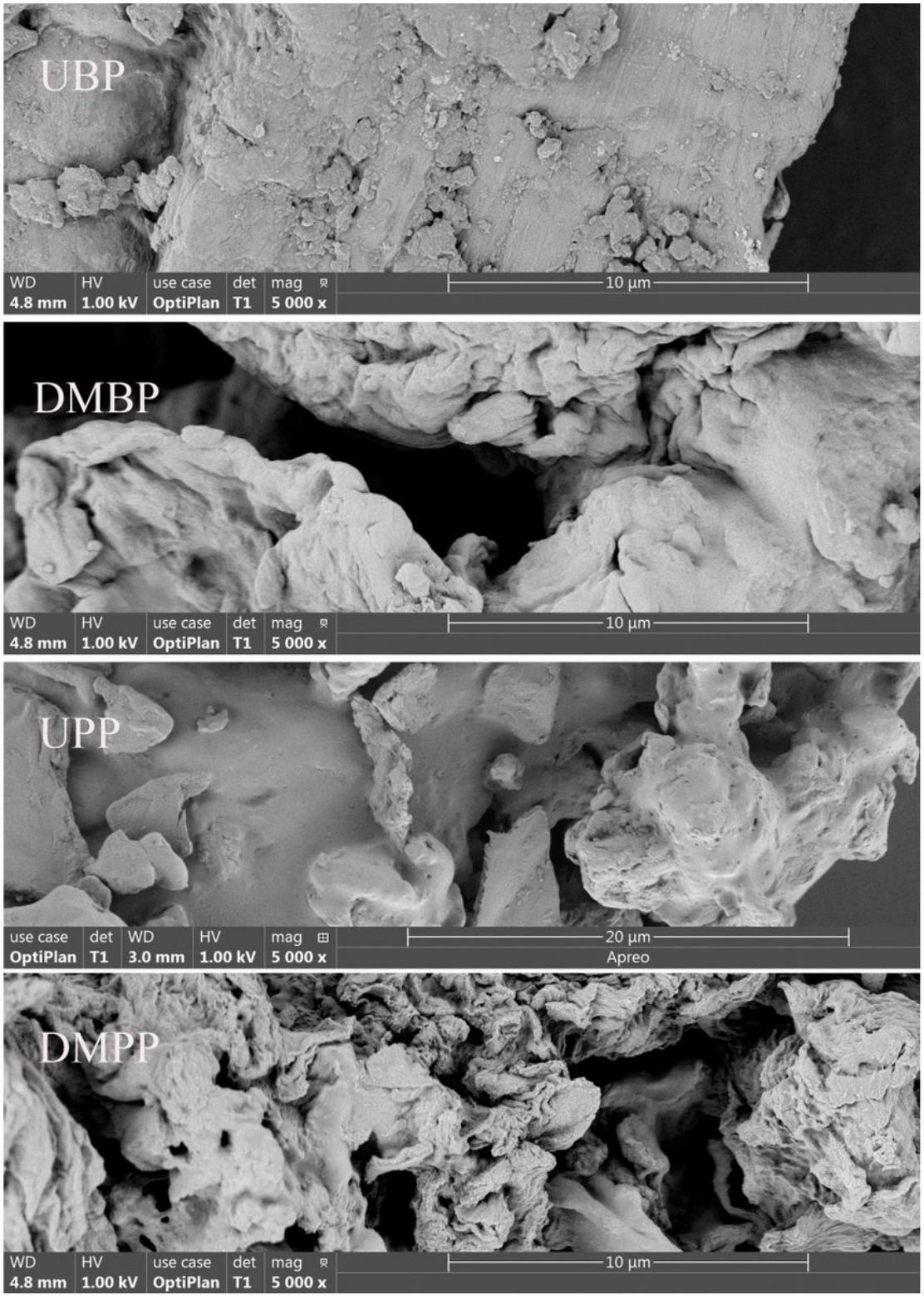

Figure 4

Surface morphology characterization of the adsorbents by SEM

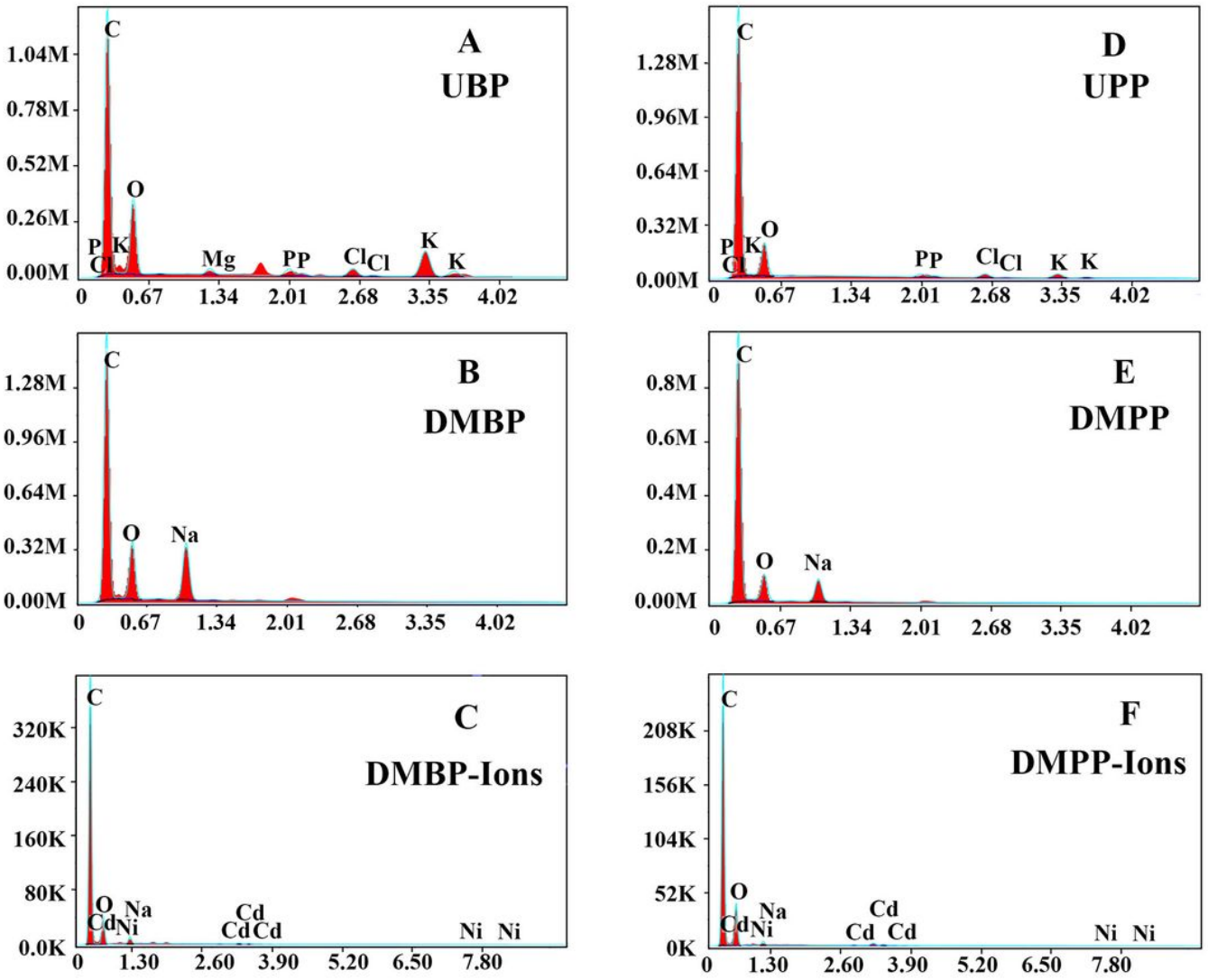

Figure 5

Surface metal ion states of the adsorbents observed by EDX. (a, d) unmodified peels, (b, e) DTPA modified peels before adsorption, (c, f) DTPA modified peels after adsorption

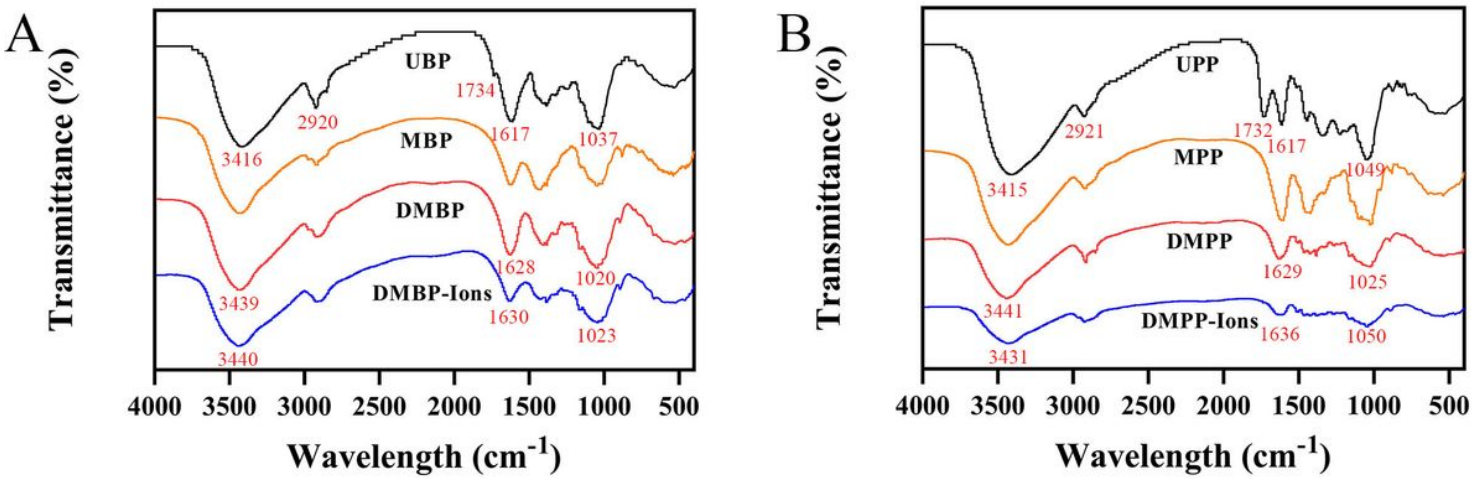

Figure 6

FTIR spectra of the adsorbents. MBP (mercerized banana peel), MPP (mercerized pomegranate peel)

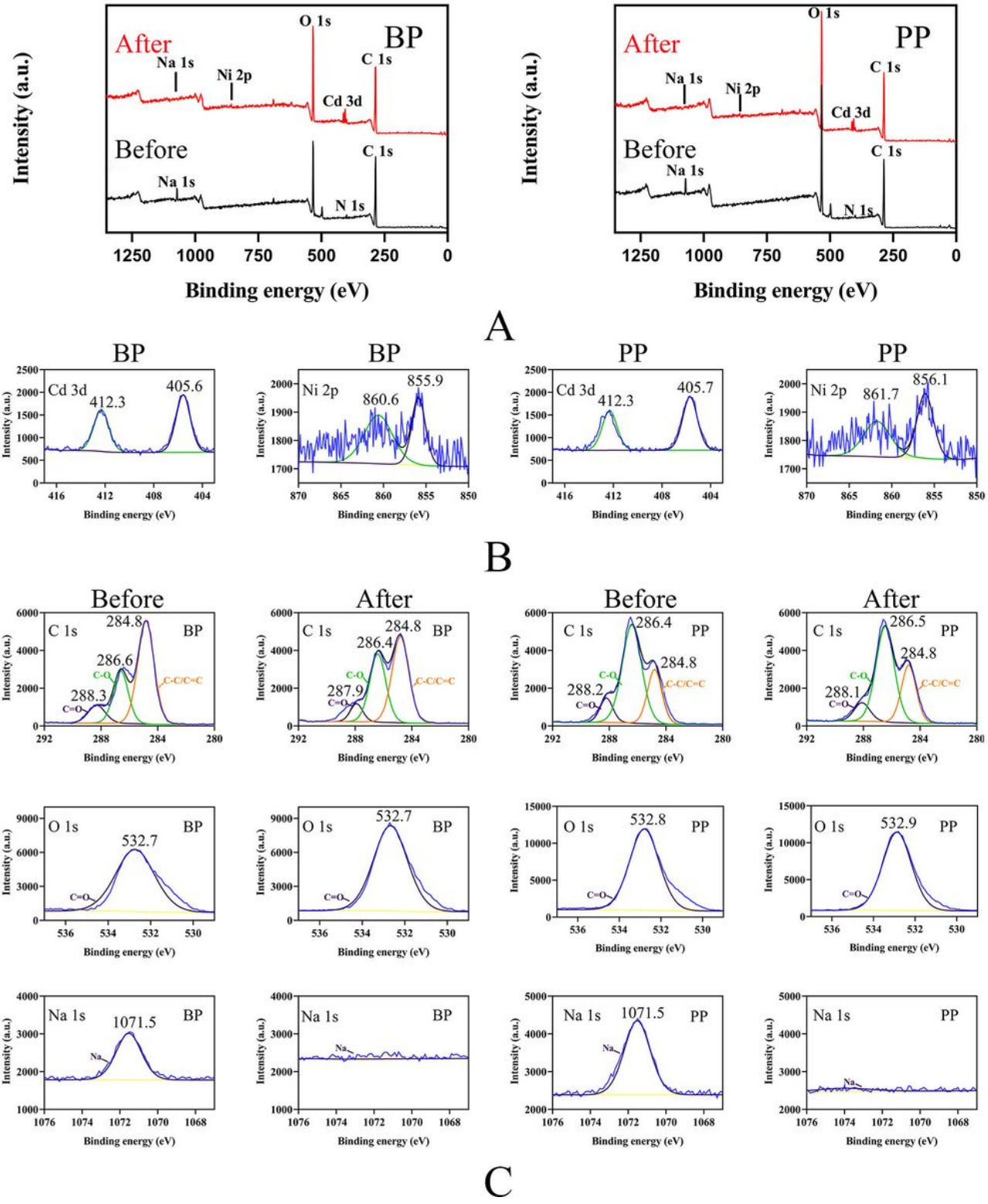

Figure 7

High-resolution XPS spectra of adsorbents. (a) full spectrum of adsorbents before and after adsorption, (b) fine spectrum of Cd and Ni after adsorption; (c) fine spectrum of C, O, Na before and after adsorption